Reaction of 16-Electron Ruthenium and Iridium Amide Complexes with Acidic Alcohols: Intramolecular C−H Bond Activation and the Isolation of Cyclometalated Complexes

Takashi Koike and Takao Ikariya*

Department of Applied Chemistry, Graduate School of Science and Engineering and Frontier Collaborative Research Center, Tokyo Institute of Technology, O-okayama, Meguro-ku, Tokyo 152-8552, Japan

Received October 13, 2004

The 16-electron transition metal amide complexes, Cp*M[κ^2(*N,N′*)-(*S,S*)-TsNCHPhCHPhNH] (M = Ir, Rh, Cp* = pentamethylcyclopentadienyl, Ts = *p*-toluenesulfonyl, Ph = C_6H_5) and Ru[κ^2(*N,N′*)-(*S,S*)-TsNCHPhCHPhNH](*p*-cymene), react with acidic alcohols, CF_3CH_2-OH or phenols, to give the corresponding alkoxide complexes, which are readily convertible to metallacycles via intramolecular C−H bond activation of the aromatic group on the diamine ligand. For example, the Ir and Rh amide complexes are transformed to the metallacycles Cp*M[κ^3(*N,N′,C*)-(*S,S*)-$CH_3C_6H_3SO_2$NCHPhCHPhNH$_2$] (M = Ir, Rh), while the Ru amide complex having structures isoelectronic with the Cp*Ir complex gives two types of metallacycles, Ru[κ^3(*N,N′,C*)-(*S,S*)-$CH_3C_6H_3SO_2$NCHPhCHPhNH$_2$](*p*-cymene) and Ru[κ^3-(*N,N′,C*)-(*S,S*)-TsNCHPhCH(C_6H_4)NH$_2$](*p*-cymene), which are formed by the C−H bond activation of an aromatic ring in either the Ts group or the diamine ligand. NMR study for the cyclometalation of the Ir amide complex with phenols suggests that the reaction proceeds through the phenoxide complexes as intermediates.

Introduction

Well-defined chiral transition metal amide complexes with metal/NH bifunctionality,[1−3] Cp*M[κ^2(*N,N′*)-(*S,S*)-TsNCHPhCHPhNH] (M = Ir (**1a**), Rh (**2a**), Cp* = pentamethylcyclopentadienyl, Ts = *p*-toluenesulfonyl, Ph = C_6H_5) and Ru[κ^2(*N,N′*)-(*S,S*)-TsNCHPhCHPhNH]-(*p*-cymene) (**3a**), have been developed as practical catalysts for asymmetric hydrogen transfer reduction[1] and C−C bond formation.[2] Thanks to sufficient Brønsted basicity originating from the metal/NH bifunctional effect, the amide complexes can effectively cleave a O−H bond of 2-propanol or formic acid and a C−H bond of acidic compounds such as nitromethane, dimethylmalonate, phenylacetylene, and acetone, giving the corresponding hydrido amine complexes and alkyl amine complexes, Cp*M(R)[κ^2(*N,N′*)-Ts-diamine] and Ru(R)[κ^2-(*N,N′*)-Ts-diamine](*p*-cymene) (M = Ir, Rh, R = H, CH_2NO_2, $CH(COOCH_3)_2$, C≡CC_6H_5, and CH_2COCH_3), respectively.[1,2] When alcohols having β-hydrogen atoms such as 2-propanol were used as acidic compounds, the reaction gave the corresponding hydrido amine complexes possibly through a pericyclic transition state,[4] in which the formation of the hydride complex from the alkoxide complex through β-H elimination was energetically unfavorable as discussed in previous papers.[4a,b] On the other hand, the reaction of the amide complex with formic acid proceeds in a stepwise manner possibly via ion pair formation, leading to the corresponding formate complex, which subsequently undergoes decarboxylation to give the hydrido amine complex with the release of carbon dioxide.[5] These results prompted us to reinvestigate the scope of the deprotonation of acidic com-

(1) (a) Hashiguchi, S.; Fujii, A.; Takehara, J.; Ikariya, T.; Noyori, R. *J. Am. Chem. Soc.* **1995**, *117*, 7562−7563. (b) Fujii, A.; Hashiguchi, S.; Uematsu, N.; Ikariya, T.; Noyori, R. *J. Am. Chem. Soc.* **1996**, *118*, 2521−2522. (c) Uematsu, N.; Fujii, A.; Hashiguchi, S.; Ikariya, T.; Noyori, R. *J. Am. Chem. Soc.* **1996**, *118*, 4916−4917. (d) Haack, K.-J.; Hashiguchi, S.; Fujii, A.; Ikariya, T.; Noyori, R. *Angew. Chem., Int. Ed. Engl.* **1997**, *36*, 285−288. (e) Hashiguchi, S.; Fujii, A.; Haack, K.-J.; Matsumura, K.; Ikariya, T.; Noyori, R. *Angew. Chem., Int. Ed. Engl.* **1997**, *36*, 288−290. (f) Mashima, K.; Abe, T.; Tani, K. *Chem. Lett.* **1998**, 1199−1200. (g) Mashima, K.; Abe, T.; Tani, K. *Chem. Lett.* **1998**, 1201−1202. (h) Murata, K.; Ikariya, T.; Noyori, R. *J. Org. Chem.* **1999**, *64*, 2186−2187. (i) Murata, K.; Okano, K.; Miyagi, M.; Iwane, H.; Noyori, R.; Ikariya, T. *Org. Lett.* **1999**, *1*, 1119−1121. (j) Mao, J.; Baker, D. C. *Org. Lett.* **1999**, *1*, 841−843. (k) Koike, T.; Murata, K.; Ikariya, T. *Org. Lett.* **2000**, *2*, 3833−3836. (l) Okano, K.; Murata, K.; Ikariya, T. *Tetrahedron Lett.* **2000**, *41*, 9277−9280. (m) Cossy, J.; Eustache, F.; Daiko, P. I. *Tetrahedron Lett.* **2001**, *42*, 5005−5007. (n) Watanabe, M.; Murata, K.; Ikariya, T. *J. Org. Chem.* **2002**, *67*, 1712−1715. (o) Hamada, T.; Torii, T.; Izawa, K.; Noyori, R.; Ikariya, T. *Org. Lett.* **2002**, *4*, 4373−4376.

(2) (a) Murata, K.; Konishi, H.; Ito, M.; Ikariya, T. *Organometallics* **2002**, *21*, 253−255. (b) Watanabe, M.; Murata, K.; Ikariya, T. *J. Am. Chem. Soc*. **2003**, *125*, 7508−7509. (c) Ikariya, T.; Wang, H.; Watanabe, M.; Murata, K. *J. Organomet. Chem.* **2004**, *689*, 1377−1381. (d) Watanabe, M.; Ikagawa, A.; Wang, H.; Murata, K.; Ikariya, T. *J. Am. Chem. Soc*. **2004**, *126*, 11148−11149.

(3) (a) Fulton, J. R.; Holland, A. W.; Fox, D. J.; Bergman, R. G. *Acc. Chem. Res.* **2002,** *35*, 44−56. (b) Fulton, J. R.; Sklenak, S.; Bouwkamp, M. W.; Bergman, R. G. *J. Am. Chem. Soc*. **2002,** *124*, 4722−4737. (c) Holland, A. W.; Bergman, R. G. *J. Am. Chem. Soc*. **2002,** *124*, 14684−14695. (d) Conner, D.; Jayaprakash, K. N.; Wells, M. B.; Manzer, S.; Gunnoe, T. B.; Boyle, P. D. *Inorg. Chem*. **2003,** *42*, 4759−4772.

(4) (a) Alonso, D. A.; Brandt, P.; Nordin, S. J. M.; Andersson, P. G. *J. Am. Chem. Soc.* **1999**, *121,* 9580−9588. (b) Yamakawa, M.; Ito, H.; Noyori, R. *J. Am. Chem. Soc.* **2000**, *122*, 1466−1478. (c) Casey, C. P.; Singer, S. W.; Powell, D. R.; Hayashi, R. K.; Kavana, M. *J. Am. Chem. Soc.* **2001**, *123*, 1090−1101. (d) Abdur-Rashid, K.; Clapham, S. E.; Hadzovic, A.; Harvey, J. N.; Lough, A. J.; Morris, R. H. *J. Am. Chem. Soc.* **2002**, *124,* 15104−15118. (e) Casey, C. P.; Johnson, J. B. *J. Org. Chem.* **2003**, *68,* 1998−2001.

(5) Koike, T.; Ikariya, T. *Adv. Synth. Catal.* **2004**, *346*, 37−41.

10.1021/om049205x CCC: $30.25
Publication on Web 01/19/2005

Scheme 1

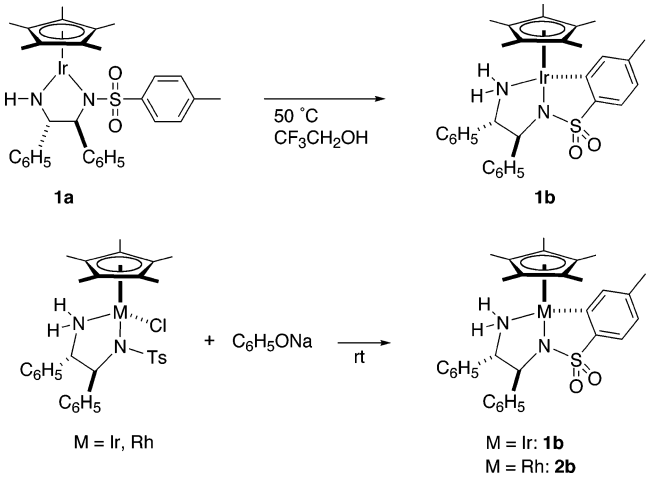

pounds with the amide complexes, and we found that the amide complexes Cp*M[κ^2(*N,N′*)-(*S,S*)-TsNCHPhCHPhNH] (M = Ir (**1a**), Rh (**2a**)) and Ru[κ^2(*N,N′*)-(*S,S*)-TsNCHPhCHPhNH](*p*-cymene) (**3a**) readily reacted with acidic alcohols, CF_3CH_2OH or phenols, to give cyclometalated complexes[6] in good to excellent yields. These complexes might be formed via intramolecular C−H bond cleavage of the aromatic ring on the Ts-diamine ligand possibly through the alkoxide complexes as intermediates.

Results and Discussion

Reaction of the Amide Complexes 1a−3a with Acidic Alcohols, CF_3CH_2OH or Phenol. The purple-colored 16-electron Ir amide complex **1a** in CF_3CH_2OH as solvent has been proven to convert at 50 °C to a yellow-colored cyclometalated complex, Cp*Ir[κ^3(*N,N′,C*)-(*S,S*)-$CH_3C_6H_3SO_2NCHPhCHPhNH_2$] (**1b**), as a single diastereomer almost quantitatively (Scheme 1).[7] The complex **1b** was also obtained by the treatment of complex **1a** in toluene with 1.1 equiv of C_6H_5OH at 50 °C. Notably, in the absence of the alcohols under otherwise identical conditions, the reaction of the complex **1a** proceeded very slowly, suggesting that the alcohol is crucial for transformation to the metallacycle **1b**. The complex **1b** can be conveniently obtained by reaction of Cp*IrCl[κ^2(*N,N′*)-(*S,S*)-TsNCHPhCHPhNH$_2$] with C_6H_5ONa in good yield (Scheme 1).

An X-ray crystallographic analysis of complex **1b**, as illustrated in Figure 1, confirmed that it has a three-legged piano stool coordination environment with Cp*, sulfonamido, amino, and tolyl ligands.[8] Crystallographic data and selected bond distances and angles are given in Table 1 and Table 2. The Ir−$C_{(metallacycle)}$, Ir−$N_{(amino)}$, and Ir−$N_{(amido)}$ distances have mean values of 2.039,[6e] 2.133, and 2.125 Å, respectively. The chirality of the (*S,S*)-diamine ligand determines the *R* configuration around the central metal, as observed in the analogous complexes.[1d,2a] NMR spectroscopic data in CD_2Cl_2 are consistent with the structure of **1b** in solution. Two nonequivalent NH protons were observed at 3.21 and 3.89 ppm because of their coordination to the chiral metal center. In the $^{13}C\{^1H\}$ NMR, six carbon peaks, due to the Ts group attached to the metallacycle ring, were observed at 136.1, 139.2, 140.4, 143.3, 147.3, and 147.4 ppm.[6e]

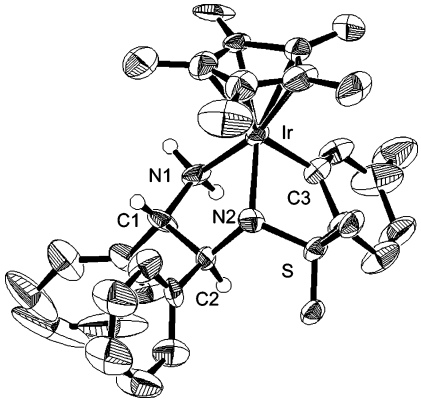

Figure 1. Structural view of Cp*Ir[κ^3(*N,N′,C*)-(*S,S*)-$CH_3C_6H_3SO_2NCHPhCHPhNH_2$] (**1b**).

An analogous Rh metallacyclic compound, Cp*Rh[κ^3-(*N,N′,C*)-(*S,S*)-$CH_3C_6H_3SO_2NCHPhCHPhNH_2$] (**2b**), could be obtained from the reaction of Cp*RhCl[κ^2(*N,N′*)-(*S,S*)-TsNCHPhCHPhNH$_2$] with C_6H_5ONa in good yield. An X-ray crystallographic analysis of complex **2b** confirmed that it has a similar structure to that of complex **1b** (see Supporting Information).[9] The Rh−$C_{(metallacycle)}$, Rh−$N_{(amino)}$, and Rh−$N_{(amido)}$ distances have mean values of 2.037, 2.123, and 2.129 Å, respectively. NMR spectroscopic data in CD_2Cl_2 are consistent with the structure of the metallacycle **2b** in solution. Two nonequivalent NH protons were observed at 2.53 and 3.04 ppm. In the $^{13}C\{^1H\}$ NMR spectrum, six carbon peaks, assigned to the Ts group attached to the central metal, were observed at 137.4, 139.9, 140.2, 144.4, 149.6, and 162.2 ppm; each signal was coupled with Rh (see Experimental Section).

When the Ru amide complex **3a**, having structures isoelectronic with the Cp*Ir complex, was treated with CF_3CH_2OH, the reaction proceeded smoothly to give a mixture of two metallacycles, Ru[κ^3(*N,N′,C*)-(*S,S*)-$CH_3C_6H_3SO_2NCHPhCHPhNH_2$](*p*-cymene) (**3b**)[10] and Ru[κ^3(*N,N′,C*)-(*S,S*)-TsNCHPhCH(C_6H_4)NH_2](*p*-cymene) (**3c**)[11] (Scheme 2). The aromatic C−H bonds, in

(6) For reviews of cyclometalation, see for example: (a) Dehand, M.; Pfeffer, M. *Coord. Chem. Rev.* **1976,** *18*, 327−352. (b) Omae, I. *Coord. Chem. Rev.* **1988**, *83*, 137−167. (c) Ryabov, A. D. *Chem. Rev.* **1990**, *90*, 403−424. (d) van der Boom, M. E.; Milstein, D. *Chem. Rev.* **2003**, *103*, 1759−1792. For cyclometalation of half-sandwich complexes, see: (e) Davies, D. L.; Al-Duaij, O.; Fawcett, J.; Giardiello, M.; Hilton, S. T.; Russell, D. R. *Dalton Trans.* **2003,** 4132−4138. The references of the related cyclometalated complexes are reported in this paper.

(7) This cyclometalation proceeds cleanly with high selectively.

(8) An X-ray crystallographic analysis of the metallacycle **1b** was performed. In Figure 1, there are omissions of the crystal solvent and the other molecule of the same structure. Crystallographic data and structure refinement parameters of complex **1b** are shown in Table 1. All hydrogen atoms were calculated from ideal geometries. See Supporting Information.

(9) An X-ray crystallographic analysis of the metallacycle **2b** was performed (see Supporting Information). Crystallographic data and structure refinement parameters of the complex **2b** are shown in Table 1.

(10) An X-ray crystallographic analysis of the metallacycles **3b** and **3c** was performed. In Figure 2 (upper view), the crystal solvent and the other type of metallacycle **3c** are omitted. Crystallographic data and structure refinement parameters of the complexes **3b** and **3c** are shown in Table 1. All hydrogen atoms were calculated from ideal geometries. See Supporting Information.

(11) An X-ray crystallographic analysis of the metallacycle **3c** was performed. In Figure 2 (bottom view), the crystal solvent is omitted. Crystallographic data and structure refinement parameters of complex **3c** are shown in Table 1. All hydrogen atoms were calculated from ideal geometries. See Supporting Information.

Table 1. Crystallographic Data for Complexes 1b, 2b, 3b, 3c, and 5b

	1b	2b	3b and 3c	3c	5b
formula	$C_{38}H_{43}IrN_2O_2S$	$C_{32.50}H_{37}N_2O_2SRhCl_3$	$C_{32}H_{36}N_2O_2SRuCl_2$	$C_{35}H_{40}F_6N_2O_4RuS$	$C_{21}H_{31}IrN_2O_2S$
fw	784.05	728.99	684.68	799.83	567.77
cryst size, mm	0.4 × 0.3 × 0.1	0.2 × 0.2 × 0.2	0.2 × 0.2 × 0.2	0.3 × 0.15 × 0.1	0.3 × 0.3 × 0.1
space group	$P2_12_12_1$(#19)	$P2_12_12_1$(#19)	$P2_1$(#4)	$P2_12_12_1$(#19)	$P2_1/n$ (#14)
a, Å	11.851(4)	19.211(3)	9.488(1)	13.333(6)	8.854(3)
b, Å	19.851(7)	29.506(5)	23.927(2)	15.768(8)	15.7638(5)
c, Å	29.288(9)	11.965(2)	13.586(3)	16.512(8)	15.134(5)
β, deg			94.39(1)		98.693(3)
V, Å^3	6889.7(39)	6782.5(21)	3075.3(9)	3471.4(29)	2087.9(12)
Z	8	8	4	4	4
ρ_{calc}, g cm^{-3}	1.512	1.428	1.479	1.530	1.806
T, K	173	123	253	173	173
μ, cm^{-1}(Mo Kα)	39.82	8.31	7.83	5.85	65.31
absorption corr	empirical	empirical	empirical	empirical	empirical
transmn factors, min./max.	0.8104/1.0000	0.8101/1.0000	1.00/1.00	0.8984/1.0000	0.4718/1.0000
$2\theta_{max}$, deg	55.0	55.0	60.1	55.0	55.0
no. of reflns measd	69 309	57 332	8817	27 251	16 336
no. of unique reflns	8611	15 548	8811	4392	4676
no. of reflns ($I > 3.00\sigma(I)$)	45 363	11 413	881[c]	14 543	4643
no. of variables	840	771	780	447	276
$R1$ ($I > 3.00\ \sigma(I)$)[a]	0.050[b]	0.087	0.055[d]	0.066	0.047
$wR2$ ($I > 3.00\sigma(I)$)[a]	0.060[b]	0.109	0.133[c]	0.169	0.255
diff Four peaks, min./max., e Å^{-3}	−5.94/8.87	−2.68/3.97	−0.96/1.25	−4.37/11.80	−3.21/1.45

[a] $R = \sum||F_o| - |F_c||/\sum|F_o|$, $wR = [\sum(w(F_o^2 - F_c^2)^2)/\sum(w(F_o^2)^2)]^{1/2}$. [b] $R = \sum||F_o| - |F_c||/\sum|F_o|$, $wR = [\sum(w(|F_o| - |F_c|)^2)/\sum(wF_o^2)]^{1/2}$. [c] $I > 0.00\sigma(I)$. [d] $I > 2.00\sigma(I)$.

Table 2. Selected Bond Distances (Å) and Angles (deg) for Complexes 1b, 2b, 3b, 3c, and 5b

	1b[a]	2b[a]	3b	3c	5b
M−N$_{(amino)}$	2.133	2.123	2.130(5)	2.140(5)	2.168(7)
M−N$_{(amido)}$	2.125	2.129	2.134(5)	2.136(4)	2.136(6)
M−C$_{(metallacycle)}$	2.039	2.037	2.069(6)	2.079(6)	2.056(7)
N$_{(amino)}$−M−N$_{(amino)}$	77.7	79.6	80.3(2)	77.7(2)	80.0(3)
N$_{(amino)}$−M−C$_{(metallacycle)}$	86.3	85.9	85.5(2)	76.9(2)	89.5(3)
N$_{(amino)}$−M−C$_{(metallacycle)}$	83.6	83.6	82.8(2)	80.8(2)	82.4(3)
M−N$_{(amino)}$−C1	108.7	107.4	107.2(3)	103.4(3)	106.7(5)
M−N$_{(amino)}$−C2	115.2	113.9	112.5(3)	114.1(3)	112.2(5)
M−N$_{(amino)}$−S	108.7	108.0	108.6(3)	125.7(3)	107.5(3)
S−N$_{(amino)}$−C2	113.1	112.7	111.6(4)	115.4(4)	117.0(6)

[a] Mean value.

Scheme 2

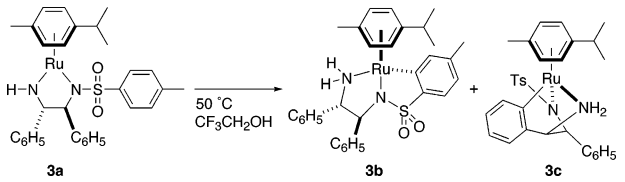

either the Ts group or the phenyl group on the diamine backbone, participated in intramolecular activation with the aid of added alcohols to facilitate metallacycle formation. The ^{1}H NMR spectrum of the reaction mixture showed that complex **3c** was formed as the major product (**3b**:**3c** = 1:4). An X-ray crystallographic analysis of the single crystals obtained by recrystallization of the crude mixture from a mixed solvent of CH_2Cl_2 and diethyl ether revealed that the crystal lattice contains two different metallacycles, **3b** and **3c**, per unit cell. ORTEP drawings for complexes **3b** and **3c** are shown in Figure 2, respectively. Complex **3b** has a three-legged piano stool structure similar to **1b** and **2b**. The Ru−C$_{(metallacycle)}$, Ru−N$_{(amino)}$, and Ru−N$_{(amido)}$ distances are 2.069(6), 2.130(5), and 2.134(5) Å, respectively. The coordination environment around the Ru atom in complex **3c** can be described as a three-legged

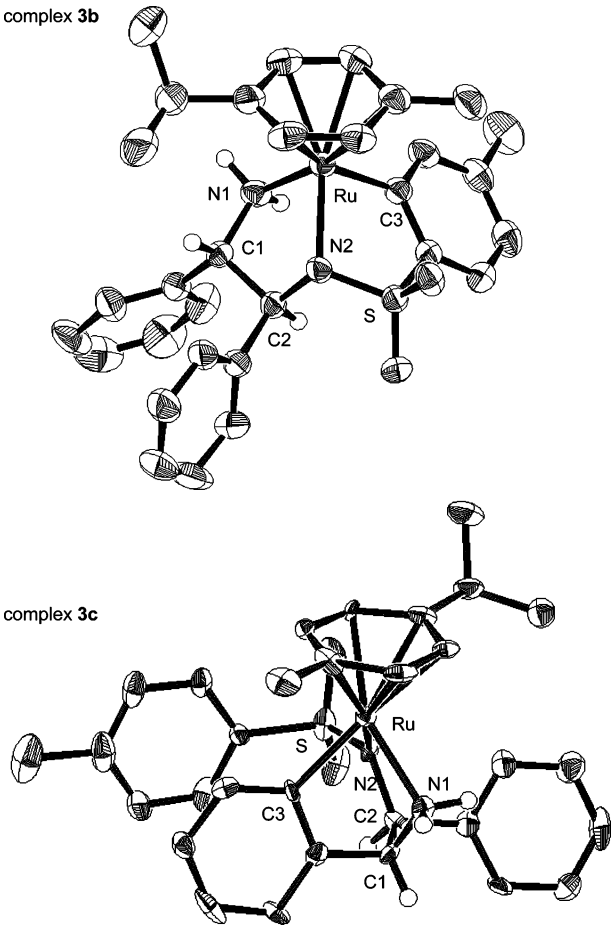

Figure 2. Structural views of complexes Ru[κ^3(*N*,*N*′,*C*)-(*S*,*S*)-$CH_3C_6H_3SO_2NCHPhCHPhNH_2$](*p*-cymene) (**3b**) and Ru[κ^3(*N*,*N*′,*C*)-(*S*,*S*)-$TsNCHPhCH(C_6H_4)NH_2$](*p*-cymene) (**3c**).

piano stool with *p*-cymene, sulfonamido, amino, and phenyl ligands. The Ru−C$_{(metallacycle)}$, Ru−N$_{(amino)}$, and Ru−N$_{(amido)}$ distances are 2.079(6), 2.140(5), and 2.136(4)

Scheme 3

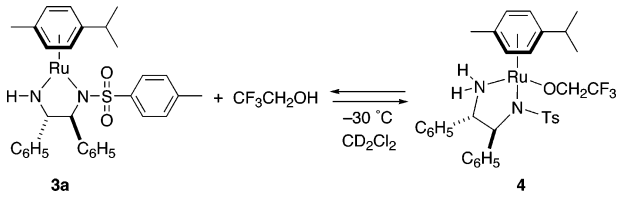

Å, respectively. NMR spectroscopic data of complexes **3b** and **3c** are consistent with the solid state structure of these complexes in solution. The ^{1}H NMR spectrum of **3c** shows nonequivalent signals for N*HH* at 2.82 and 3.34 ppm. The ^{13}C{^{1}H} NMR spectrum of isolated **3c** displays six carbon peaks derived from a phenyl group bonded to the Ru metal center.

Reaction of the Amide Complex with 1 Equiv of CF_3CH_2OH: Attempts to Isolate the Metal Alkoxide Complexes. On the basis of the experimental results discussed above, alkoxide or phenoxide complexes could be possible intermediates in the metallacycle formation. The ^{1}H NMR spectrum of a CD_2Cl_2 solution containing the Ir amide complex **1a** and 1 equiv of CF_3CH_2OH in an NMR tube gave no signals that could be assigned to the corresponding alkoxide complex even at low temperature, possibly because the reversible reaction was too rapid to detect the alkoxide complex under the conditions for NMR study. However, in the reaction of Ru complex **3a** with CF_3CH_2OH, the ^{1}H NMR spectrum of a reaction mixture of **3a** and 1 equiv of CF_3CH_2OH in an NMR tube gave a set of broad signals at room temperature. On cooling the purple-colored reaction mixture below −30 °C, the color of the solution changed to orange and the spectrum displayed a mixture of the starting amide complex **3a**, the alkoxide complex, Ru(OCH_2CF_3)[κ^2(*N,N′*)-(*S,S*)-TsNCHPhCHPhNH$_2$](*p*-cymene) (**4**), and unreacted CF_3CH_2OH (Scheme 3). The ^{1}H NMR spectrum of the alkoxide complex **4** in CD_2Cl_2 at −30 °C displays two doublet quartets due to the diastereotopic methylene protons of the OC*HH*CF_3 group at 4.20 and 4.63 ppm, respectively (see Supporting Information), indicating that the alcohol oxygen bonds to the chiral metal center. An increase in the amount of added alcohol caused an increase in the signals due to the alkoxide complex, indicating that the alkoxide complex **4** existed in a temperature-dependent equilibrium with **3a** and free CF_3CH_2OH. These results showed that the reverse reaction from the alkoxide to amide complexes is facile because an intramolecular deprotonation of very acidic NH protons of the alkoxo amine complexes bearing the basic metal-OR units[3a] rapidly proceeds to form the amide complexes in solution.

Although alkoxide complexes could not be isolated from the reaction of **1a** or **3a** with CF_3CH_2OH, an analogous Ir alkoxide complex having no NH protons in the diamine ligand, Cp*Ir(OCH_2CF_3)[κ^2(*N,N′*)-TsNCH$_2$CH$_2$N(CH$_3$)$_2$] (**5a**), was isolable from the reaction of the Ir chloride complex, Cp*IrCl[κ^2(*N,N′*)-TsNCH$_2$CH$_2$N(CH$_3$)$_2$], with CF_3CH_2OH containing a base, KO*t*-Bu. The structure of **5a** was confirmed by NMR spectroscopy as well as X-ray crystallographic analysis.[12] The ^{1}H NMR spectrum of **5a** in CD_2Cl_2 shows two signals due to the methyl proton of the N(C*H*$_3$)$_2$ group at 2.66 and 2.97 ppm and two doublet quartets assigned to the

Scheme 4

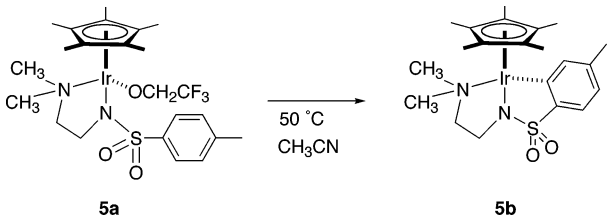

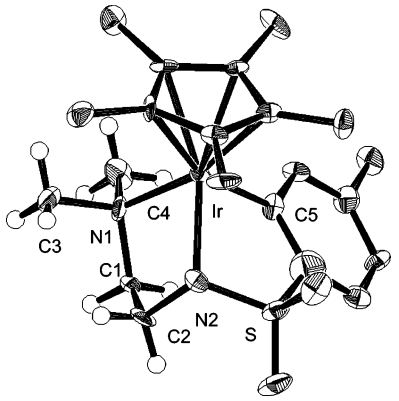

Figure 3. Structural view of Cp*Ir[κ^3(*N,N′,C*)-$CH_3C_6H_3SO_2NCH_2CH_2N(CH_3)_2$] (**5b**).

methylene protons of OC*HH*CF_3 at 4.07 and 4.34 ppm. These spectroscopic data were consistent with the nitrogen and oxygen being bound to the chiral metal center on the NMR time scale. The analogous Ru alkoxide complex, Ru(OCH_2CF_3)[κ^2(*N,N′*)-TsNCH$_2$CH$_2$N(CH$_3$)$_2$](*p*-cy-mene) (**6a**), was isolable in a manner similar to the Ir complex. The structure of **6a** was also confirmed by NMR spectroscopy and X-ray crystallographic analysis (see Supporting Information).[13]

It should be noted that the isolable Ir alkoxide complex **5a** was found to undergo intramolecular cyclometalation at 50 °C, leading to the metallacycle product Cp*Ir[κ^3(*N,N′,C*)-$CH_3C_6H_3SO_2NCH_2CH_2N(CH_3)_2$] (**5b**), as shown in Scheme 4 and Figure 3.[14] An X-ray crystallographic analysis of the complex **5b** confirmed that it has a three-legged piano stool coordination environment. The Ir−$C_{(mettallacycle)}$, Ir−$N_{(amino)}$, and Ir−$N_{(amido)}$ distances are 2.056(7), 2.168(7), and 2.136(6) Å, respectively. The ^{1}H NMR spectrum of **5b** shows nonequivalent signals, 3.21 and 3.89 ppm in CD_2Cl_2, for N(C*H*$_3$)$_2$. This nonequivalence is consistent with the expected structure in which the nitrogen can coordinate to the chiral metal center on the NMR time scale. The

(12) An X-ray crystallographic analysis of the alkoxide complex **5a** was performed. Crystal and structure refinement parameters of complex **5a**: $C_{24}H_{36}F_3IrN_2O_3SCl_2$, M_r = 752.74, triclinic, space group $P\bar{1}$ (# 2), a = 8.1777(9) Å, b = 8.6253(4) Å, c = 21.909(2) Å, V = 1439.9(2) Å^3, Z = 2, D_c = 1.736 g/cm^3, μ(Mo Kα) = 49.54 cm^{-1}, T = 193 K, R_1 (wR_2) = 0.095 (0.249) for 9967 observed reflections ($I > 3.00\sigma(I)$). All hydrogen atoms were calculated from ideal geometries. See Supporting Information.

(13) An X-ray crystallographic analysis of the alkoxide complex **6a** was performed. Crystal and structure refinement parameters of complex **6a**: $C_{23}H_{33}F_3N_2O_3RuS$, M_r = 575.65, triclinic, space group $P\bar{1}$(# 2), a = 8.56(6) Å, b = 12.32(10) Å, c = 13.11(10) Å, V = 1253.1(16) Å^3, Z = 2, D_c = 1.525 g/cm^3, μ(Mo Kα) = 7.58 cm^{-1}, T = 173 K, R_1 (wR_2) = 0.078 (0.182) for 3704 observed reflections ($I > 3.00\sigma(I)$). All hydrogen atoms were calculated from ideal geometries. See Supporting Information.

(14) An X-ray crystallographic analysis of the metallacycle **5b** was performed. Crystallographic data and structure refinement parameters of complex **5b** are shown in Table 1. All hydrogen atoms were calculated from ideal geometries. See Supporting Information.

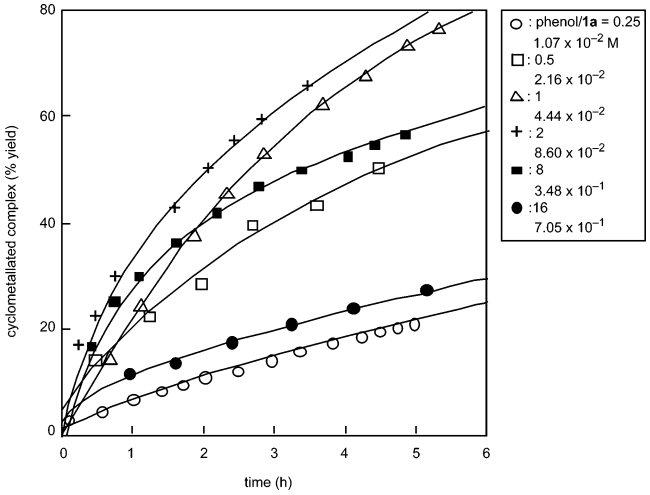

Figure 4. Time dependence of the concentration of *p*-$CF_3C_6H_4OH$.

^1H NMR spectrum shows only three proton signals due to the Ts group of **5b**. The $^{13}C\{^1H\}$ NMR spectrum displays six carbon signals derived from the Ts group as observed in complexes **1b** and **2b**.

A Possible Mechanism for the Cyclometalation of the Amide Complex in the Presence of Phenols. As discussed in the previous section, the addition of the acidic alcohol, CF_3CH_2OH or phenol, facilitated C−H bond activation to give cyclometalation products. Trifluoromethyl-substituted phenol, *p*-$CF_3C_6H_4OH$ (**7**), with stronger acidity than CF_3CH_2OH, promoted the cyclometalation; monitoring the profile of the reaction of **1a** with **7**, determined by NMR spectroscopy, provided a deeper insight into the reaction pathways. Figure 4 shows the time dependence curves of the yield of the cyclometalation product **1b** as a function of the concentration of **7** at 50 °C in CD_3CN. Noticeably, the reaction profiles show a complex dependency on the concentration of the phenol. Because of the intricacy of the reaction profiles, full analysis of the reaction kinetics could not be performed. It should be noted that the reaction of **1a** with 0.25 equiv of *p*-$CF_3C_6H_4OH$ **7** to **1a** (1.07×10^{-2} M) proceeded very slowly but reached complete conversion to give the product **1b** after 3 days. The rate of the reaction increases with the concentration of **7** but reaches a maximum at about 2 equiv (8.60×10^{-2} M) of **1a**. After the maximum is reached, the reaction is strongly retarded by the addition of a large amount of **7**, suggesting that free *p*-$CF_3C_6H_4OH$ possibly interacts with the basic phenoxo complex **8** via hydrogen bonding to form a stabilized adduct **9**[15] as shown in Scheme 5. The hydrogen bonding interaction of **7** might cause reduction of the basicity of the complex **8**, leading to the resting stage of the reaction as shown in Scheme 5.

An ^{19}F NMR spectrum of a reaction mixture containing the Ir amide complex **1a** and 1 equiv of *p*-$CF_3C_6H_4OH$ (**7**) shows two broad signals at −60.5 and −61.2 ppm at −90 °C. On increasing the temperature to room temperature, a sharp singlet was observed at −62.1 ppm, which is close to the position for the free phenol

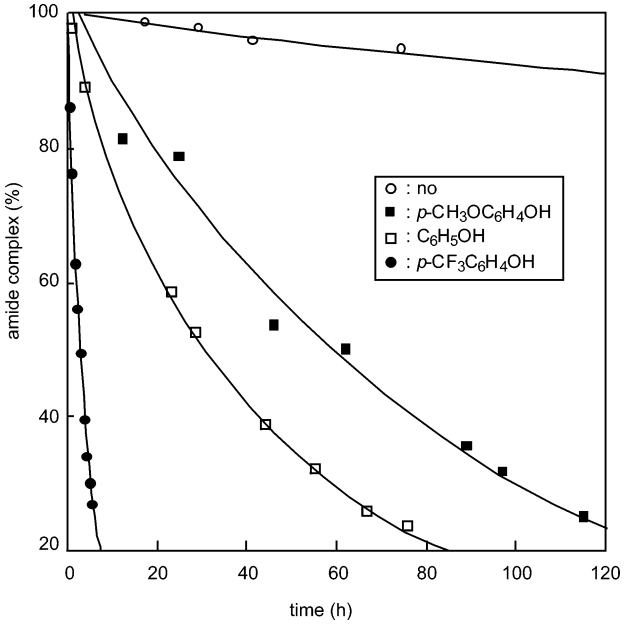

Figure 5. Dependence of the phenol's substituent on the reaction rate.

Scheme 5

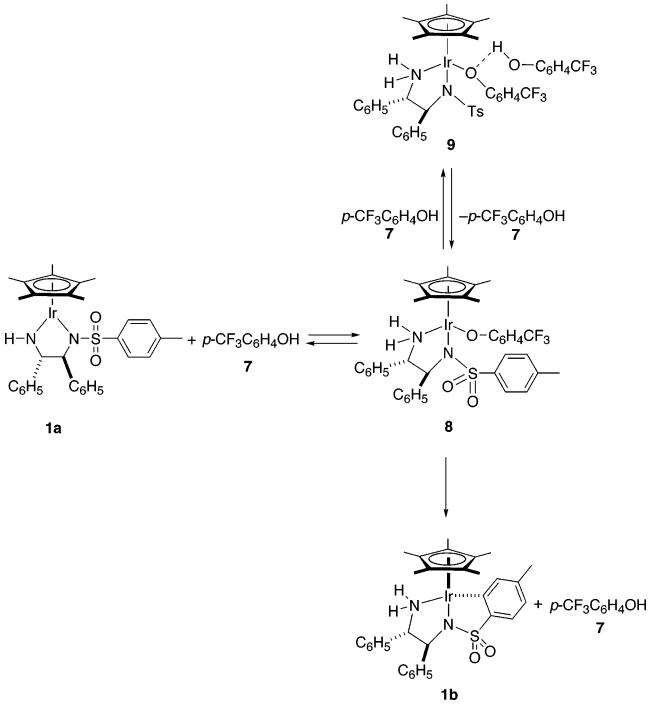

7, showing that phenoxide complex **8** existed in an equilibrium with the amide complex **1a** and free phenol, as observed in the reaction of **1a** with CF_3CH_2OH (Scheme 5). The use of a large excess of **7** to **1a** gave only one broad ^{19}F signal around 62.0 ppm even at −90 °C, suggesting that a rapid exchange reaction between the phenoxo ligand of **8** and free *p*-$CF_3C_6H_4OH$ possibly takes place via **9** under the reaction conditions.

Monitoring the reaction of Ir amide complex **1a** with 1 equiv of various phenols by the disappearance of the signals due to **1a**, in the ^1H NMR spectra at 50 °C in CD_3CN, revealed the transformation profile shown in Figure 5. It should be noted that the phenol's substituent has a significant effect on the rate of the cyclo-

(15) (a) Kegley, S. E.; Schaverien, C. J.; Freudenberger, J. H.; Bergman, R. G. *J. Am. Chem. Soc.* **1987**, *109*, 6563−6565. (b) Kim, Y. J.; Osakada, K.; Takenaka, A.; Yamamoto, A. *J. Am. Chem. Soc.* **1990,** *112*, 1096−1104.

metalation, as the conversion rate of **1a** increases in the order *p*-$CH_3OC_6H_4OH$ < C_6H_5OH < *p*-$CF_3C_6H_4OH$. In the absence of phenols under otherwise identical conditions, the reaction proceeded very slowly, indicating that the presence of the alcoholic compounds could facilitate the reaction and the phenoxo complex might be involved in the rate-limiting step in the present transformation.

Based on these experimental results, the overall reaction pathways of the cyclometalation promoted by alcohols are described in Scheme 5. The cyclometalation proceeds possibly through the phenoxide complex **8**, which exists in a temperature-dependent equilibrium with the amide complex **1a**, the free phenol, and the adduct **9**. At a low phenol concentration compared to **1a**, the reaction rate depends on the concentration of both phenol and complex **1a**, in which the formation of adduct **9** was minimized at an early stage in the reaction. Electronic tuning of the substituents on the phenols significantly affects the rate of the reaction, while the transformation of **1a** to **1b** is strongly inhibited by a large amount of the phenol because of the formation of kinetically stable adduct **9**. Then, the cyclometalation irreversibly proceeds to the thermodynamically stable metallacycle. There are three possible C−H activation pathways from the phenoxide complex **8**, leading to the metallacycle **1b**: (1) the dissociation of the alkoxo anion leading to an ion pair intermediate,[5] followed by electrophilic substitution,[16] and generation of a vacant site either by dissociation of the NH_2 ligand or by ring-slippage, followed by either (2) concerted activation[6e,17] with the aid of the metal−OR bond or (3) the oxidative addition of the aromatic C−H bond. Further investigations including details of the reaction kinetics as well as computational analysis on the reaction pathways are still required.

Conclusions

We have shown intramolecular orthometalation promoted by the metal alkoxide intermediates derived from the 16-electron amide complexes and acidic alcohols. The Brønsted basicity of the amide complex as well as the alkoxide intermediate contribute to the C−H bond activation. However, the present intramolecular C−H bond activation irreversibly proceeds to give the stable cyclometalated complex, which is an inactive species for catalytic asymmetric reduction[1] and C−C bond formation.[2] The fine-tuning of the structures as well as electronic factors in the chiral amide catalysts are crucial for attaining superior catalyst performance in terms of reactivity and selectivity.

Experimental Section

All experiments were conducted under an argon atmosphere using Schlenk techniques. All deuterated NMR solvents were dehydrated and degassed by appropriate methods. Amide complexes **1a** and **3a** and chloro complexes were prepared according to reported procedures.[1d,g,h] ^{1}H and ^{13}C NMR were recorded on a JEOL JNM-LA300 Fourier transform spectrometer. X-ray single-crystal structural analysis studies were made on a Rigaku Saturn or Rigaku RAXIS CS using graphite-monochromated Mo Kα radiation (λ = 0.71070 Å). Elemental analysis was performed on a Perkin-Elmer 2400II CHNS/O or LECO CHNS-932.

Cp*Ir[κ^3(*N,N′,C*)-(*S,S*)-$CH_3C_6H_3SO_2NCHPhCHPhNH_2$] (1b). (a) The Ir amide complex **1a** (1.20×10^{-1} g, 1.73×10^{-4} mol) in CF_3CH_2OH (3.5 mL) was stirred at 50 °C for 7.5 h. The solvent was removed under reduced pressure. The resulting product was almost quantitatively Cp*Ir[κ^3(*N,N′,C*)-(*S,S*)-$CH_3C_6H_3SO_2NCHPhCHPhNH_2$] (**1b**). Recrystallization from CH_2ClCH_2Cl afforded crystals. Isolated yield: 23%. (b) To a toluene solution (3 mL) of the Ir amide complex **1a** (1.08×10^{-1} g, 1.56×10^{-4} mol) was added a toluene solution (0.18 mL) of C_6H_5OH (1.47×10^{-2} g, 1.56×10^{-4} mol). The reaction was conducted at 50 °C. After 2 days, the product was recrystallized from toluene. Cp*Ir[κ^3(*N,N′,C*)-(*S,S*)-$CH_3C_6H_3SO_2NCHPhCHPhNH_2$] (**1b**) was obtained for isolated yield, 51%. ^{1}H NMR (300.4 MHz, CD_2Cl_2, rt, δ/ppm): 1.79 (s, 15H; $C_5(CH_3)_5$), 2.29 (s, 3H; *p*-$CH_3C_6H_3SO_2N$), 3.21 (br dd, 1H; *p*-$CH_3C_6H_3SO_2NCHPhCHPhNH$*H*), 3.65 (m, 1H; *p*-$CH_3C_6H_3SO_2NCHPhCH$*H*$PhNH_2$), 3.89 (br, 2H; *p*-$CH_3C_6H_3SO_2NCH$*H*$PhCHPhNH$*H*), 6.78−7.37 (13H; *p*-$CH_3C_6H_3SO_2NCH(C_6H_5)CH(C_6H_5)NH_2$). ^{13}C{^{1}H} NMR (75.6 MHz, CD_2Cl_2, rt, δ/ppm): 9.2 ($C_5(CH_3)_5$), 21.5 (*p*-$CH_3C_6H_3SO_2N$), 69.6, 76.2 (*p*-$CH_3C_6H_3SO_2NCHPhCHPhNH_2$), 87.9 ($C_5(CH_3)_5$), 124.6−147.4 (*p*-$CH_3C_6H_3SO_2NCH(C_6H_5)CH(C_6H_5)NH_2$). Anal. Calcd. for $C_{31}H_{35}O_2N_2S_1Ir_1$: C 53.81, H 5.10, N 4.05, S 4.63. Found: C 53.87, H 5.07, N 4.01, S 4.41.

Cp*Rh[κ^3(*N,N′,C*)-$CH_3C_6H_3SO_2NCHPhCHPhNH_2$] (2b). To a CH_2Cl_2 solution (5 mL) of Cp*RhCl[κ^2(*N,N′*)-TsNCHPhCHPhNH$_2$] (1.01×10^{-1} g, 1.58×10^{-4} mol) was added $C_6H_5ONa{\cdot}3H_2O$ (3.20×10^{-2} g, 1.88×10^{-4} mol). The reaction was conducted at room temperature for 2 days. The reaction mixture was filtered through filter paper. Recrystallization from CH_2Cl_2 and diethyl ether afforded the yellow crystals. Isolated yield: 15%. ^{1}H NMR (300.4 MHz, CD_2Cl_2, rt, δ/ppm): 1.76 (s, 15H; $C_5(CH_3)_5$), 2.38 (s, 3H; *p*-$CH_3C_6H_3SO_2N$), 2.53 (br dd, 1H; *p*-$CH_3C_6H_3SO_2NCHPhCHPhNH$*H*), 3.04 (br d, 1H; *p*-$CH_3C_6H_3SO_2NCHPhCHPhNH$*H*), 3.78 (m, 2H; *p*-$CH_3C_6H_3SO_2NCH$*H*$PhCH$*H*$PhNH_2$), 6.77−7.35 (13H; *p*-$CH_3C_6H_3SO_2NCH(C_6H_5)CH(C_6H_5)NH_2$). ^{13}C{^{1}H} NMR (75.6 MHz, CD_2Cl_2, rt, δ/ppm): 9.4 ($C_5(CH_3)_5$), 21.6 (*p*-$CH_3C_6H_3SO_2N$), 69.7, 72.8 (*p*-$CH_3C_6H_3SO_2NCHPhCHPhNH_2$), 95.4 (d, $^1J_{RhC}$ = 6.5 Hz; $C_5(CH_3)_5$), 124.9−129.0 (*p*-$CH_3C_6H_3SO_2NCH(C_6H_5)CH(C_6H_5)NH_2$), 137.4, 139.9, 140.2, 144.4, 149.6, 162.2 (each d, J_{RhC} = 1.1, 1.1, 1.5, 0.8, 1.5, 32.4 Hz, respectively; *p*-$CH_3C_6H_3SO_2N$). Anal. Calcd for $C_{31}H_{35}O_2N_2S_1Rh_1$: C 61.79, H 5.85, N 4.65, S 5.32. Found: C 62.03, H 6.07, N 4.53, S 5.14.

Ru[κ^3(*N,N′,C*)-(*S,S*)-$CH_3C_6H_3SO_2NCHPhCHPhNH_2$](*p*-cymene) (3b) and Ru[κ^3(*N,N′,C*)-(*S,S*)-TsNCHPhCH(C_6H_4)NH_2](*p*-cymene) (3c). The Ru amide complex **3a** (9.11×10^{-2} g, 1.52×10^{-4} mol) in CF_3CH_2OH (3.5 mL) was stirred at 50 °C for 7.5 h. The solvent was removed under reduced pressure. (a) Recrystallization from CH_2Cl_2 and diethyl ether afforded yellow crystals including the metallacycles **3b** and **3c**. It was determined by X-ray analysis. (b) Recrystallization from CF_3CH_2OH afforded the metallacycle **3c**. Isolated yield: 27%.

Spectral data for 3b. ^{1}H NMR (300.4 MHz, CD_2Cl_2, rt, δ/ppm): 1.29 (dd, 6H; $CH_3C_6H_4CH(CH_3)_2$), 2.21, 2.38 (each s, 3H; $CH_3C_6H_4CH(CH_3)_2$, *p*-$CH_3C_6H_3SO_2N$), 2.38 (br, 1H; *p*-$CH_3C_6H_3SO_2NCHPhCHPhNH$*H*), 2.96 (m, 1H; $CH_3C_6H_4CH(CH_3)_2$), 3.52 (d, $^3J_{HH}$ = 11 Hz, 1H; *p*-$CH_3C_6H_3SO_2NCHPhCH$*H*$PhNH_2$), 3.96 (m, 1H; *p*-$CH_3C_6H_3SO_2NCH$*H*$PhCHPhNH_2$), 4.01 (br, 1H; *p*-$CH_3C_6H_3SO_2NCHPhCHPhNH$*H*), 4.92, 5.36, 5.45 (4H; $CH_3C_6H_4CH(CH_3)_2$), 6.70−7.52 (13H; *p*-$CH_3C_6H_3SO_2NCH(C_6H_5)CH(C_6H_5)NH_2$).

Spectral data for 3c. ^{1}H NMR (300.4 MHz, CD_2Cl_2, rt, δ/ppm): 0.95 (d, $^3J_{HH}$ = 7.1 Hz, 3H; $CH_3C_6H_4CH(CH_3)(CH_3)$), 1.25 (d, $^3J_{HH}$ = 6.8 Hz, 3H; $CH_3C_6H_4CH(CH_3)(CH_3)$), 2.26, 2.39 (each s, 3H; $CH_3C_6H_4CH(CH_3)_2$, *p*-$CH_3C_6H_4SO_2N$), 2.82 (br, 1H; TsNCHPhCH(C_6H_4)NH*H*), 2.96 (m, 1H; $CH_3C_6H_4CH(CH_3)_2$),

(16) (a) Sommer, J.; Bukala, J. *Acc. Chem. Res.* **1993,** *26*, 370−376. (b) Jia, C.; Kitamura, T.; Fujiwara, Y. *Acc. Chem. Res.* **2001,** *34*, 633−639.

(17) Oxgaard, J.; Muller, R. P.; Goddard, W. A., III; Periana, R. A. *J. Am. Chem. Soc.* **2004**, *126*, 352−363.

3.34 (br, 1H; TsNCHPhCH(C_6H_4)N*H*H) 4.02 (br s, 1H; TsNCHPhC*H*(C_6H_4)NH_2), 4.10 (br s, 1H; TsNC*H*PhCH(C_6H_4)-NH_2), 5.09, 5.14, 5.52 (4H; $CH_3C_6H_4CH(CH_3)_2$), 6.68−7.73 (13H; *p*-$CH_3C_6H_4SO_2NCH(C_6H_5)CH(C_6H_4)NH_2$). $^{13}C\{^1H\}$ NMR (75.6 MHz, CD_2Cl_2, rt, δ/ppm): 18.5, 21.3, 21.8, 23.8, 30.3 ($CH_3C_6H_4CH(CH_3)_2$, *p*-$CH_3C_6H_4SO_2N$), 63.3, 69.9 (TsNCHPhCH-(C_6H_4)NH_2), 78.1, 82.1, 82.4, 88.5, 99.8, 107.6 ($CH_3C_6H_4CH$-$(CH_3)_2$), 126.1−167.5 (*p*-$CH_3C_6H_4SO_2NCH(C_6H_5)CH(C_6H_4)$-$NH_2$). Anal. Calcd for $C_{31}H_{34}O_2N_2S_1Ru_1\cdot(CF_3CH_2OH)_{1.75}$: C 53.48, H 5.11, N 3.62, S 4.14. Found: C 53.26, H 5.41, N 3.70, S 3.97.

Cp*Ir(OCH$_2$CF$_3$)[κ^2(*N,N*′)-TsNCH$_2$CH$_2$N(CH$_3$)$_2$] (5a). To a CF_3CH_2OH solution (4 mL) of Cp*IrCl[κ^2(*N,N*′)-TsNCH$_2$-$CH_2N(CH_3)_2$] (1.17×10^{-1} g, 1.94×10^{-4} mol) was added KO*t*-Bu (2.89×10^{-2} g, 2.56×10^{-4} mol). The reaction was conducted at room temperature overnight. The solvent was removed under reduced pressure. Toluene was added to the residue,. The toluene solution was filtered through filter paper. Recrystallization from CH_2Cl_2 and hexane afforded yellow crystals. Isolated yield: 48%. These crystals were air-sensitive. ^1H NMR (300.4 MHz, CD_2Cl_2, rt, δ/ppm): 1.55−1.72, 2.68−2.97 (m, 4H; TsNC*H*$_2$C*H*$_2$N(CH_3)$_2$), 1.57 (s, 15H; $C_5(CH_3)_5$), 2.38 (s, 3H; *p*-C*H*$_3$C$_6$H$_4$SO$_2$N), 2.66 (s, 3H; N(CH_3)(C*H*$_3$)), 2.97 (s, 3H; N(C*H*$_3$)(CH_3)), 4.07 (m, 1H; $CF_3CHHOIr$), 4.34 (m, 1H; $CF_3CHHOIr$), 7.22 (d, $^3J_{HH}$ = 7.8 Hz, 2H; *p*-$CH_3C_6H_2H_2SO_2N$), 7.66 (d, $^3J_{HH}$ = 8.1 Hz, 2H; *p*-$CH_3C_6H_2H_2SO_2N$). ^{19}F NMR (282.65 MHz, CD_2Cl_2, rt, δ/ppm): −77.0 (dd, C*F*$_3$CH$_2$OIr). Anal. Calcd for $C_{23}H_{34}O_3N_2S_1F_3Ir_1$: C 41.37, H 5.13, N 4.19. Found: C 40.94, H 5.58, N 4.14.

Cp*Ir[κ^3(*N,N*′,*C*)-CH$_3$C$_6$H$_3$SO$_2$NCH$_2$CH$_2$N(CH$_3$)$_2$] (5b). To a CF_3CH_2OH solution (3.5 mL) of Cp*IrCl[κ^2(*N,N*′)-TsNCH$_2$-$CH_2N(CH_3)_2$] (1.15×10^{-1} g, 1.89×10^{-4} mol) was added KO*t*-Bu (2.76×10^{-2} g, 2.46×10^{-4} mol). The reaction was conducted at room temperature. After 12 h, the solvent was removed under reduced pressure. The residue was the alkoxide complex **5a**. Then, CH_3CN (5 mL) was added to the alkoxide complex **5a** and stirred at 50 °C overnight. The reaction mixture was filtered through filter paper. Recrystallization from CH_3CN afforded pale yellow crystals. Isolated yield: 16%. ^1H NMR (300.4 MHz, CD_2Cl_2, rt, δ/ppm): 1.45, 1.90, 3.00, 3.55 (m, 4H; *p*-$CH_3C_6H_3SO_2NCH_2CH_2N(CH_3)_2$), 1.60 (s, 15H; C_5-$(CH_3)_5$), 2.29 (s, 3H; *p*-C*H*$_3C_6H_3SO_2$), 2.58 (s, 3H; N(C*H*$_3$)(CH_3)), 3.05 (s, 3H; N(CH_3)(C*H*$_3$)), 7.18, 7.21, 7.40 (m, each 1H; *p*-$CH_3C_6H_3SO_2N$). $^{13}C\{^1H\}$ NMR (75.6 MHz, CD_2Cl_2, rt, δ/ppm): 9.3 ($C_5(CH_3)_5$), 21.4 (*p*-$CH_3C_6H_3SO_2N$), 52.2, 53.3, 57.0, 66.7 (*p*-$CH_3C_6H_3SO_2NCH_2CH_2N(CH_3)(CH_3)$), 88.5 ($C_5(CH_3)_5$), 122.9, 124.2, 138.7, 139.2, 146.6, 150.3 (*p*-$CH_3C_6H_3SO_2N$). Anal. Calcd for $C_{21}H_{31}O_2N_2S_1Ir_1$: C 44.42, H 5.50, N 4.93, S 5.65. Found: C 44.31, H 5.43, N 4.83, S 5.41.

Ru(OCH$_2$CF$_3$)[κ^2(*N,N*′)-TsNCH$_2$CH$_2$N(CH$_3$)$_2$] (6a). To a CF_3CH_2OH solution (3.5 mL) of RuCl[κ^2(*N,N*′)-TsNCH$_2$CH$_2$N-$(CH_3)_2$](*p*-cymene) (1.07×10^{-1} g, 2.08×10^{-4} mol) was added KO*t*-Bu (2.67×10^{-2} g, 2.38×10^{-4} mol). The reaction was conducted at room temperature for 12 h. The solvent was then removed under reduced pressure. Toluene was added to the residue. The reaction mixture was filtered through filter paper. Recrystallization from CH_2Cl_2 and diethyl ether afforded yellow crystals. Isolated yield: 37%. ^1H NMR (300.4 MHz, CD_2-Cl_2, rt, δ/ppm): 1.22 (dd, 6H; $CH_3C_6H_4CH(CH_3)_2$), 1.50 (m, 1H; TsNCH$_2$CH*H*N(CH_3)$_2$), 2.11, 2.37, 2.68, 2.94 (each s, 3H; C*H*$_3$C$_6$H$_4$CH(CH_3)$_2$, *p*-C*H*$_3$C$_6$H$_4$SO$_2$NCH$_2$CH$_2$N(C*H*$_3$)(C*H*$_3$)), 2.49, 2.85, 2.90 (each m., 1H; TsNC*H*$_2$C*H*HN(CH_3)$_2$), 5.11, 5.22, 5.51, 5.66 (4H; $CH_3C_6H_4CH(CH_3)_2$), 7.22 (d, $^3J_{HH}$ = 8.1 Hz, 2H; *p*-$CH_3C_6H_2H_2SO_2N$), 7.68 (d, $^3J_{HH}$ = 8.1 Hz, 2H; *p*-$CH_3C_6H_2H_2$-SO_2N). ^{19}F NMR (282.65 MHz, CD_2Cl_2, rt, δ/ppm): −77.0 (dd, C*F*$_3$CH$_2$ORu). Anal. Calcd for $C_{23}H_{33}O_3N_2S_1F_3Ru_1$: C 47.99, H 5.78, N 4.87, S 5.57. Found: C 48.04, H 6.03, N 4.80, S 5.48.

Experimental Procedure for Cyclometalation of Iridium Amide Complex 1a with *p*-CF$_3$C$_6$H$_4$OH. A CD_3CN solution of 1 equiv of *p*-$CF_3C_6H_4OH$ **7** (2.15×10^{-5} mol) was added to a solution of complex **1a** (1.47×10^{-2} g, 2.12×10^{-5} mol), dihexyl ether (2×10^{-3} mL) as internal standard, and CD_3CN (0.46 mL) in an NMR tube. The tube was sealed and the resultant metallacycle **1b** was traced by ^1H NMR at 323.15 K. The resulting reaction profile is shown in Figure 4. In a similar manner, the reaction of the amide complex **1a** with 0.25, 0.5, 2, 8, and 16 equiv of *p*-$CF_3C_6H_4OH$ **7** (1.07×10^{-2}, 2.16×10^{-2}, 8.60×10^{-2}, 3.48×10^{-1}, 7.05×10^{-1} M) gave transformation profiles as shown in Figure 4.

Experimental Procedure for Cyclometalation of Iridium Amide Complex 1a Using Various Phenols. A CD_3-CN solution of 1 equiv of C_6H_5OH (1.80×10^{-2} mL, 1.89 × 10^{-5} mol) was added to a solution of the Ir amide complex **1a** (1.28×10^{-2} g, 1.85×10^{-5} mol), dihexyl ether (2×10^{-3} mL) as internal standard, and CD_3CN (0.4 mL) in an NMR tube. The tube was sealed and the disappearing amide complex **1a** was traced by ^1H NMR at 323.15 K. The resulting reaction profile is shown in Figure 5. In a similar manner, the reaction of the Ir amide complex **1a** with *p*-$CH_3OC_6H_4OH$ or no alcohol gave transformation profiles as shown in Figure 5.

Acknowledgment. This work was financially supported by a grant-in-aid from the Ministry of Education, Science, Sports and Culture of Japan (No. 12305057, 14078209) and partially supported by The 21st Century COE Program. K.T. gratefully acknowledges financial support from a JSPS Research Fellowship for Young Scientists. X-ray crystallographic measurement of complex **2b** was supported by Rigaku Corporation.

Supporting Information Available: NMR data of the Ru alkoxide complex **4** and X-ray crystallographic data of **1b**, **2b**, **3b**, **3c**, **5a**, **5b**, and **6a**. This material is available free of charge via the Internet at http://pubs.acs.org.

OM049205X